Microwave Spectroscopy in Oxford: The Early Years
Remarks on the Occasion of Receiving the 1983 ISMAR Award

B. Bleaney

The Clarendon Laboratory
Parks Road
Oxford OX1 3PU United Kingdom

I. INTRODUCTION

The first measurements of spectra at microwave frequencies using modern techniques were made before the end of World War II. The reason for this was that the frequency of 24 GHz (a wavelength of 12.5 mm; known as "K-band") had been picked by the Radiation Laboratory at M.I.T. for a precision radar system. Unfortunately, it turned out that this coincided with the region at which attenuation in the atmosphere becomes a serious problem. The attenuation arises mainly from water vapor (the H_2O molecule has an electric dipole moment), and to a lesser extent from oxygen (oxygen molecules have a magnetic dipole moment). The attenuation is small, amounting to about 0.2 decibel per km at the partial pressure of water vapor normally present in the atmosphere. This is very small by laboratory standards, but in terms of a radar system aimed at detecting an echo from a distance of 50 km (a return path of 100 km), the return signal is reduced in power by a factor of 100, a very significant loss.

II. MICROWAVE ABSORPTION IN THE ATMOSPHERE

An absorption of order 0.2 db per km is extremely difficult to measure in the open atmosphere, though an ingenious radiometer was developed for this purpose at the Radiation Laboratory, M.I.T. by Dicke (1,2). It is almost equally difficult to measure in the laboratory, but a novel type of apparatus was developed by Becker and Autler (3) at Columbia University, New York, specifically for this purpose. The

absorption is small for a number of reasons. There is of course the well known fact that the quantum of energy involved is much smaller than the Boltzmann energy kT ($h\nu/kT$) being about 0.004 at room temperature for a frequency of 25 GHz; the stimulated emission and absorption are almost equal, and the net absorption is reduced by a factor ($h\nu/kT$). Since the quantum absorption is $h\nu$, the power absorption coefficient falls as the square of the frequency, a problem that arises in nearly all radiofrequency spectroscopy (an exception is electron paramagnetic resonance, EPR, below a temperature of 1 K). In addition: (1) the water vapor absorption arises from a weak transition between two excited levels with a low Boltzmann factor of about 0.12 at room temperature; and (2) at atmospheric pressure the collision frequency is not much smaller than the resonant frequency, so the absorption line is broad, and correspondingly weak.

The results obtained by Becker and Autler are shown in Figure 1. The absorption has a maximum, arising from the water vapor line, very close to the K-band frequency of 0.8 cm^{-1}; there is also a background absorption that rises steadily with increasing frequency. This is attributed to the low frequency tails of absorption lines centered at higher frequencies, and its value in the region shown in the figure depends on the widths and shapes of these lines. At atmospheric pressure, the linewidth is dominated completely by the effects of collisions with other molecules, and Van Vleck and Weisskopf (4) reconsidered the formulae of Lorentz for collision broadening when the collision frequency is comparable to the resonance frequency. In addition to the square of the frequency mentioned above, the line shape contains a "shape factor"

$$F(\nu_0, \nu) = (1/\pi) \left[\frac{\Delta\nu}{\Delta\nu^2 + (\nu_0 - \nu)^2} + \frac{\Delta\nu}{\Delta\nu^2 + (\nu_0 + \nu)^2} \right] \quad (1)$$

where the first term is similar to that of Lorentz, and the second term is important only for broad lines. The
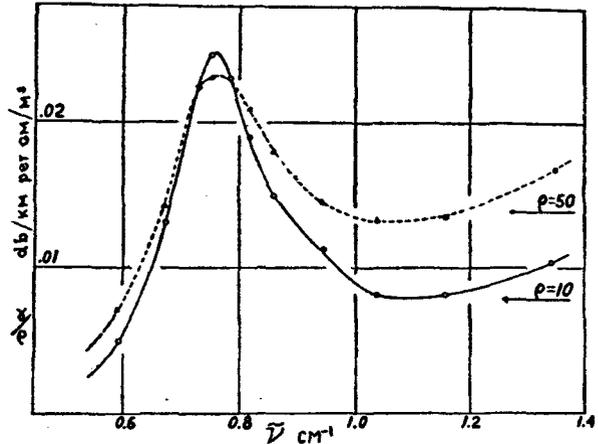
Figure 1. Absorption curve for water vapor in the atmosphere. The attenuation in db per km per g per m^3 of H_2O is plotted against wavenumber. The broken curve is for a density of 50 g/m^3, the full curve for 10 g/m^3. The increasing absorption at the higher wavenumbers arises from the tails of lines at higher frequencies. After Becker and Autler (3).

absorption coefficient at frequency ν is given by the relation

$$\alpha = n\frac{4\pi^3\nu^2}{3ckT} |\mu_{ij}|^2 F \quad (2)$$

where n is the number of molecules per unit volume in the pair of levels between which transitions are induced at resonant frequency ν_0, with transition matrix element μ_{ij}.

Because of the importance of this formula, I proposed at the beginning of 1945 that it should be checked using the microwave absorption spectrum of the ammonia molecule, NH_3. This molecule gives an absorption stronger by a factor of 1000 than that of water vapor in the atmosphere, and since the vapor pressure of ammonia at room temperature is about 6 atm, it can be studied over a wide range of pressure. With the agreement of our employers, the British Board of Admiralty, R. P. Penrose and I began such experiments early in 1945.

III. THE INVERSION SPECTRUM OF AMMONIA

The origin of the NH_3 spectrum is quite different from that of H_2O or O_2. The shape of the NH_3 molecule is a flat pyramid, with the nitrogen atom at the apex, on either side of an equilateral triangle of protons. Separating these two equilibrium configurations, there is only a rather low potential barrier, and the molecule tunnels through this barrier at a frequency of about 24 GHz. Since the direction of the electric dipole moment (1.45 Debye units) is reversed each time the barrier is traversed, there is a strong oscillating dipole moment that can interact with a microwave electric field. In 1934 Clee-
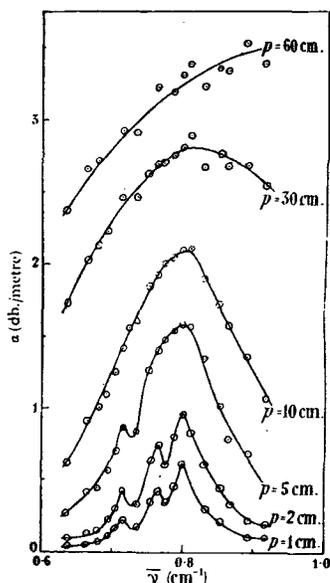

Figure 2. The inversion spectrum of ammonia gas at cm wavelengths, showing the absorption curves (in db/m) for ammonia gas at various pressures (in cm Hg). Structure becomes visible at the lower pressures. After Bleaney and Penrose (6).

ton and Williams (5) had observed the absorption using a cloth bag filled with ammonia gas; this was placed in the path of the radiation from some split-anode magnetrons, whose wavelength was measured by an echelette grating rather like a Venetian blind. They had obtained an answer that proved to be not far from that given by our modern techniques; these included waveguides, tunable reflex klystrons (designed and constructed in the Clarendon Laboratory), and silicon-tungsten diodes as detectors. In our first experiments the ammonia was contained in a 1 m length of waveguide, closed by thin mica windows. The absorption was determined from the drop in power reaching the detector when ammonia gas was admitted to the guide, and the results (6) are shown in Figure 2. As the pressure is reduced, the absorption line beomes narrower and signs of structure become visible in the spectrum; to examine this more closely, it was necessary to go to lower pressures, and to improve the sensitivity a cavity resonator was used instead of the waveguide. This cavity, shown in Figure 3, had been designed for wavelength measurements, and it was adapted by incorporating thin mica windows. The damping of the cavity on admitting the ammonia gas was determined by tuning from one half-power point of the resonance curve to the other, the motion of the micrometer drive being amplified by a simple optical lever. The "Q" of the cavity approached 10,000, and it was equivalent to use of a guide of length $Q/2\pi$ wavelengths, so that the gain in sensitivity is considerable.

The spectrum of ammonia (7) obtained at a pressure of 1.2 mm Hg is shown in Figure 4. It displays a complex structure; this arises from centrifugal distortion of the molecule when rotating. This distortion modifies the potential barrier, with a consequent change in the tunnelling frequency, that becomes slightly different for each rotational state. "End-over-end" rotation increases the height of the barrier, and decreases the tunnelling frequency; the reverse happens when the molecule rotates about its symmetry axis, a line through the nitrogen atom, perpendicular to the plane containing the protons.

The splitting was expected to follow the formula of Sheng, Dennison, and Barker (8)
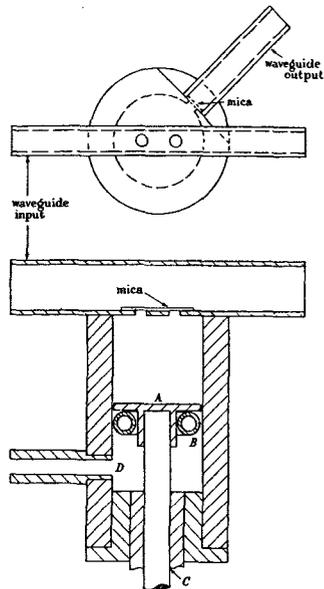
Figure 3. The cavity resonator used by Bleaney and Penrose (7) to measure the absorption of ammonia gas at lower pressures. The side view (above) shows the two-hole coupling used to select the H_{01} (TE$_{01}$) mode that gives the highest quality factor Q. A similar resonator was used to measure the wavelength. A: plunger driven by micrometer; B: water in glass tube to eliminate unwanted modes; C: oil seal; D: to reservoir of ammonia gas.

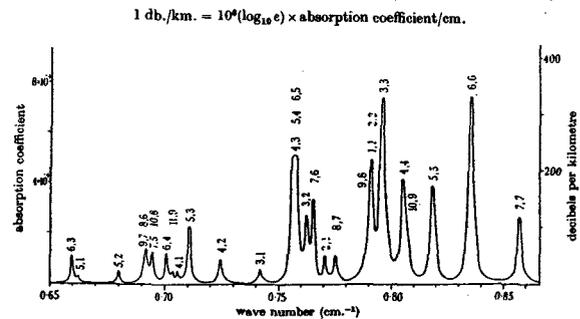1 db./km. = $10^5(\log_{10} e)$ × absorption coefficient/cm.

Figure 4. Absorption coefficient (per cm of path length) for the inversion spectrum of ammonia gas at a pressure of 1.2 mm Hg, measured by Bleaney and Penrose (7). The linewidth is about 10^{-3} cm^{-1}, and wholly due to collision broadening (the Doppler width is about 10^{-6} cm^{-1}). Each line arises from a different rotational level and is labelled by the rotational quantum numbers J, K. For K = J the molecule is rotating about its symmetry axis, and centrifugal distortion lowers the potential barrier, increasing the inversion frequency. For K << J, the molecule is rotating "end over end", increasing the barrier height and reducing the inversion frequency. The frequencies of the lines are fitted to Eq. (4) in the text.

$$\bar{\nu} = \bar{\nu}_0 - AJ(J + 1) + BK^2 \qquad (3)$$

and the formula used by us (7) was

$$\bar{\nu} = 0.7935 - 0.00505\, J(J + 1)$$

$$+ 0.00704\, K^2$$

$$+ 0.63[-0.0050\, J(J + 1)$$

$$+ 0.0070\, K^2]^2 \qquad (4)$$

in units of wavenumber (cm^{-1}). The higher order terms correspond simply to the expansion of an exponential for the tunnelling frequency.

The reason why such accurate measurements of the ammonia spectrum were possible is readily seen from the intensity. The strongest lines in Figure 4 correspond to an attenuation approaching 400 db/km instead of 0.2 db/km for water vapor in the atmosphere. The integrated absorption at a pressure of 4.5 mm Hg between wavenumbers 0.67 and 0.87 cm^{-1} agreed with the calculated value within 1%, but the extensive rotational structure makes it difficult to verify the line shape of Van Vleck and Weisskopf in detail. The linewidths vary considerably from line to line and are noticeably larger than would be expected from kinetic theory values of the collision cross-section, being mainly determined by dipolar interactions between the molecules. A

further complication is that as the pressure increases towards 1 atm, multiple collisions become important, and the resonant frequency appears to shift downwards [see Bleaney and Loubser (9)], reaching zero at a pressure of about 2 atm.

The alternative to working at high pressures is to reduce the pressure to the point at which lines from different rotational states no longer overlap. This means working in a region where the second term in the shape factor is negligible; then, at the center of a line where $(\nu - \nu_0)$ is zero, the formula for the intensity reduces to

$$\alpha = \frac{4\pi^2 \nu^2}{3ckT}|\mu_{ij}|^2 \ (n/\Delta\nu) \ . \tag{5}$$

Since the linewidth parameter $\Delta\nu$ is proportional to the collision frequency, and hence to the pressure, and the number density of molecules n is also proportional to the pressure, this formula shows that the intensity at the center of the line should be independent of pressure, so long as no other contribution to the linewidth is significant. An experimental test (10) to this prediction is shown in Figure 5. As the pressure decreases, the intensity at the center of the line at first remains constant, as expected, but then starts to decrease at a pressure well above that at which other forms of broadening should begin to play a role. The figure shows that the effect is much worse at a higher power level in the cavity, confirming that it arises from "power saturation". This effect is much worse in a cavity than in a waveguide, because the radiation density is proportional to "Q". An unfortunate result is that we were defeated in our efforts to use Stark modulation in the cavity, because this needs such a low pressure that saturation effects greatly reduce the intensity.

The use of a cavity resonator has a second drawback: a sharply tuned device is tedious if not impossible to use in searching for a weak absorption line whose frequency is not precisely known. Apart from the ammonia spectrum, only the lowest rotational lines of molecules such as OCS occur at wavelengths longer than 1 cm, and investigations of
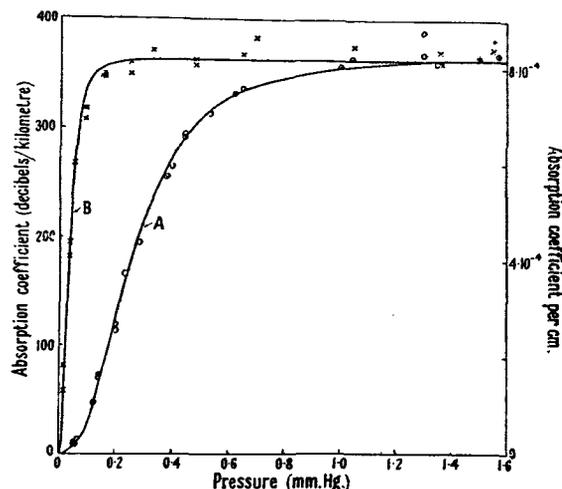

Figure 5. The absorption coefficient for ammonia gas at the center of the strongest line J,K = 3,3, as a function of pressure. The fall in absorption at the lowest pressure arises from power saturation, and occurs at higher pressures when the radiation energy density is large (curve A, power entering cavity = 12 milliwatts) than for a lower density (curve B, power = 20 microwatts). After Bleaney and Penrose (10).

their spectra were being intensively pursued in the USA. [For an authoritative treatise, see Townes and Schawlow (11)]. In 1947 Penrose and I decided to turn our efforts to electron paramagnetic resonance, a subject much more closely linked with low temperature physics, the principal research activity in the Clarendon Laboratory at that time. Paramagnetic resonance experiments had just begun at room temperature, and we decided to extend these to lower temperatures (see below, section V).

IV. FERROMAGNETIC RESONANCE

In 1945 J. H. E. Griffiths decided to investigate the permeability of the ferromagnetic metals iron, cobalt and nickel at microwave frequencies. It was already known from reflectivity measurements that the oscillatory

permeability drops to unity at optical frequencies, but there was little sign of any decrease at radiofrequencies. To make measurements at centimeter wavelengths he used a resonant cavity in which one end wall was made of the ferromagnetic metal. The power loss depends on the product of the resistivity ρ and the magnetic permeability μ, because the skin depth depends on the permeability. The power loss is measured by the damping of the cavity resonance, and to separate the effect of the permeability from other losses, he measured the change in the damping as a function of external magnetic field. As magnetic saturation in the metal is approached, the permeability decreases to unity, while the resistivity should be independent of magnetic field. Unexpectedly, the cavity losses, instead of decreasing steadily, passed through a maximum, as shown in Fig. 6, where the quanity $(\mu\rho)$ is plotted as a function of magnetic field. The figure shows that at a shorter wavelength the maximum shifts to higher field. Griffiths (12) realized that this was a resonance phenomenon, and that it did not occur exactly at the electron spin resonance point

$h\nu = g\mu_B B$, with g = 2

because of the presence of demagnetizing fields inside the metal sample. The problem of how to allow for such fields was solved using classical theory by Kittel (13), and using quantum theory by Van Vleck (14). Ferromagnetic resonance, and its later analogues antiferromagnetic and ferrimagnetic resonance, have been extensively used to investigate magnetically ordered materials.

V. ELECTRON PARAMAGNETIC RESONANCE

The discovery of ferromagnetic resonance, and of nuclear magnetic resonance by Bloch and Purcell, suggested at once that magnetic resonance could be observed in electronic paramagnetic crystals. In fact such an experiment had already been carried out by Zavoisky (15) at Kazan in the U.S.S.R., though this did not become known to us until later. His experiments,
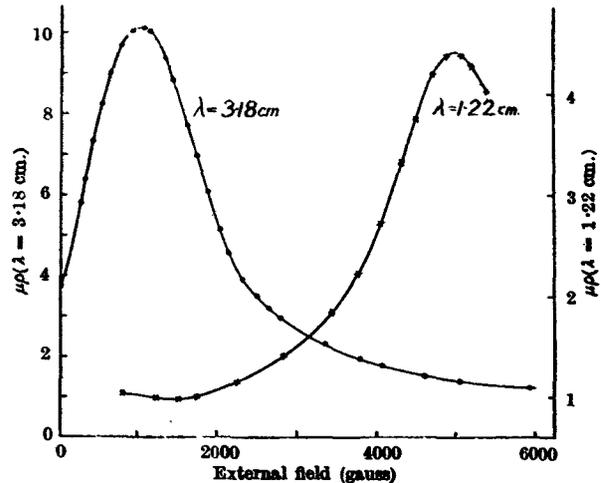

Figure 6. Ferromagnetic resonance curves of nickel metal at wavelengths of 3.18 and 1.22 cm, observed by Griffiths (12). The absorption is proportional to the product of the magnetic permeability μ and electric resistance ρ, and was determined by measuring the damping coefficient of the cavity as the applied magnetic field was increased. For higher frequencies the resonance is shifted to higher fields, but is displaced from the true resonance value by the internal field.

initially on solutions of manganese and copper salts at room temperature, were made at a frequency of 120 MHz. We were in the happy position of being able to work at frequencies 100 times greater, so that the resonance lines were much better resolved and much more intense. From pre-war use of paramagnetic salts for magnetic cooling we were aware that substances such as the alums of iron and chromium had ground states with splittings of a few GHz, and it was obvious that these could be measured by magnetic resonance with much greater precision than could be inferred from classical magneto-thermal experiments. Furthermore, large single crystals of such alums, and other substances such as copper sulphate, could readily be grown from aqueous solution. The first electron paramagnetic

resonance experiments in Oxford were carried out by D. M. S. Bagguley in the autumn of 1946 at a wavelength of 3 cm. These quickly revealed the main features of ESR: anisotropic g-values, showing different spectra when the crystal unit cell contains ions on sites where the principal axes of the g-tensor are differently oriented; splittings in zero magnetic field, caused by higher order effects of the crystal field and spin-orbit coupling, when the ground state has a degeneracy greater than two-fold [see, for example, Bagguley and Griffiths (16)]; linewidths ranging from 0.01 to over 0.1 tesla, arising from spin-spin interactions between the magnetic ions; absence of resonance at room temperature for ions whose spin-lattice relaxation rates exceed 10 to 100 GHz.

The presence of exchange interactions between the magnetic ions in insulating crystals, in addition to magnetic dipolar interactions, was suspected but little quantitative information was available. In magnetic resonance, an effect known as "exchange narrowing" was predicted by Gorter and Van Vleck (17), and this was shown to occur in $CuSO_4,5H_2O$ by Bagguley and Griffiths (18). Such a narrow resonance line is shown in Figure 7; the linewidth is only 3mT, a factor tenfold smaller than that calculated from the formulae of Van Vleck (19) for purely magnetic dipole interaction. In addition, the line shape is close to Lorentzian (exchange narrowing has similarities with motional narrowing) rather than Gaussian, the shape expected (in a good approximation) for dipolar interactions.

The resonance line in Figure 7 is observed when the applied magnetic field has a particular crystallographic direction such that the resonance lines from the two dissimilar ions in the unit cell are coincident. In other directions two resonance lines should appear because the g-value of each ion is anisotropic (g varies with angle from about 2.05 to 2.4 for the divalent cupric ion), and the principal axes of the g-tensor are different for the two ions. However, Bagguley and Griffiths (18) found that only one line appeared at a wavelength of 3.04 cm, but that at
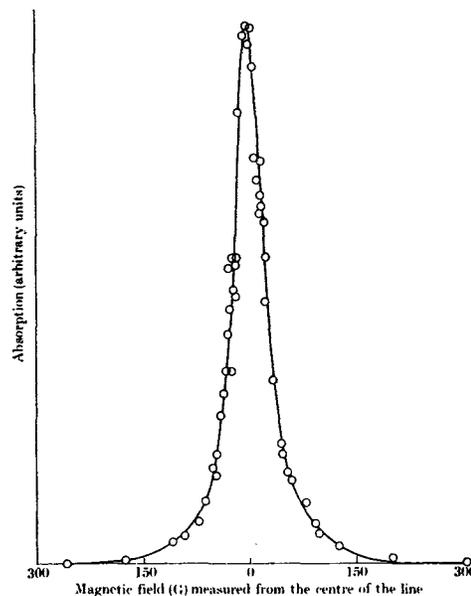

Figure 7. Electron paramagnetic resonance curve for $CuSO_4,5H_2O$ at a wavelength of 1.23 cm (frequency 24 GHz), in a direction where the line from the two copper ions in the unit cell have the same value of the spectroscopic splitting factor g. The linewidth is about one-tenth of that expected from magnetic dipole interaction between neighboring ions, showing the effect of "exchange narrowing". After Bagguley and Griffiths (18).

a shorter wavelength (0.85 cm) this was replaced by a pair of rather wide lines. This result is another effect of exchange interaction (Pryce 20). At the longer wavelength (lower field) the frequencies at which the two ions precess differ by an amount that is less than the exchange frequency; the ions are so strongly coupled that only one line is observed, at a frequency corresponding to the average of the two precession frequencies. As the applied field increases the difference between these two precession frequencies also increases, and when it approaches the exchange frequency, two lines become resolved. From these experiments an exchange frequency of about 0.15 cm^{-1}

was deduced for the Cu^{2+} ions in copper sulphate.

To overcome the problem of excessive broadening from rapid spin-lattice relaxation, measurements at lower temperatures were needed, and Penrose and I designed a simple resonant cavity, fed either by coaxial lines (for 3 cm wavelength) or waveguides (for 1.25 cm wavelength), that could be immersed in liquid oxygen or liquid hydrogen. It was then found that compounds of divalent cobalt ions $3d^7$ yielded spectra with exceedingly anisotropic g-values, and that for many compounds the small crystal field splittings were temperature dependent. For example, the divalent Ni^{2+} ion, $3d^8$, in nickel fluosilicate [see Penrose and and Stevens (21)] has a zero-field splitting of trigonal symmetry that decreases from -0.5 cm^{-1} at room temperature to -0.12 cm^{-1} at temperatures below 20 K. A survey of results for the 3d group was published in two papers by Bagguley, Bleaney, Griffiths, Penrose, and Plumpton (22).

VI. HYPERFINE STRUCTURE IN EPR

At the invitation of Professor G. J. Gorter, Penrose spent about six months at the Kamerlingh Onnes Laboratorium, Leiden, in 1948-9. There he discovered hyperfine structure in a dilute double sulfate of copper, in which 99% of the copper ions were replaced by magnesium. The hyperfine structure consisted of $(2I + 1) = 4$ lines, corresponding to the known spins $I = 3/2$ of the stable copper isotopes. Tragically, Penrose contracted a brain tumor, and died in hospital in Leiden on 28 April 1949, at the age of 28. His discovery was reported in a short letter to Nature [Penrose (23)], composed by Gorter, and in a following letter, Abragam and Pryce (24) pointed out that the anisotropy observed by Penrose in the hyperfine structure was not consistent with that expected from theory. A similar but more dramatic difficulty presented itself in the same year, when an extensive hyperfine structure was observed in dilute compounds of manganese (see 25, 26). The Mn^{2+} ion has the configuration $3d^5$, ^6S; for such a half-filled shell there is no orbital momentum, and the distribution of electronic spin

magnetism, to a good approximation, has spherical symmetry. There should therefore be no hyperfine field at the nucleus, but in fact a large hyperfine structure is observed, of nearly the same size for a range of manganese compounds. It was shown by Abragam and Pryce (27) that this arose from a finite spin density at the nucleus, resulting from exchange interaction between the inner shells of electrons and the the polarized 3d shell. This interaction causes the inner sub-shells with parallel spins to be displaced by a small amount, opposite to that for the sub-shells with anti-parallel spins. The difference is minute, but an electron in an inner s-shell produces a very large hyperfine field at the nucleus; thus for the two electrons with opposite spin orientations in the same s-shell the cancellation of the fields at the nucleus is no longer exact when they are displaced radially. This phenomenon of "core polarization" has proved to be present for all paramagnetic ions, in varying degree (it is considerably smaller in the 4f group than in the 3d group). For ions such at Cu^{2+} it accounts for the discrepancy in the magnetic hyperfine interaction mentioned above.

The spectrum of the cupric ion provided several further points of interest:

(a) "Forbidden" transitions, corresponding to changes in the nuclear magnetic quantum number, were observed by Ingram (28). These arise from the presence of a nuclear electric quadrupole interaction that competes with the magnetic hyperfine interaction when the external magnetic field is in a direction such that the magnetic hyperfine field at the nucleus is not parallel to the electric field gradient. The presence of such weak transitions is shown in Figure 8 for a dilute double sulfate of copper (29) in which further reduction of the linewidth is obtained by replacing the protons in the water of crystallization by deuterons.

(b) In a cubic crystalline field with a distortion of trigonal symmetry the orbital ground state of the cupric ion is doubly degenerate, and allowing
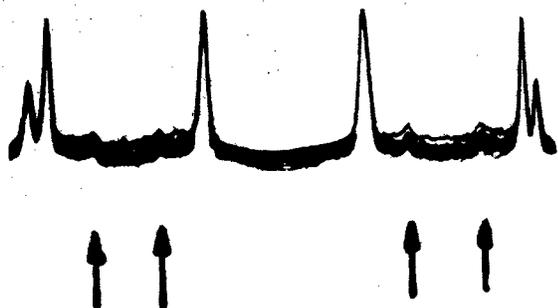
Figure 8. Hyperfine structure of the two copper isotopes ^{63}Cu, ^{65}Cu in a heavily diluted double sulfate of copper, $K_2(Zn,Cu)(SO_4)_2,6D_2O$. The $(2I+1) = 4$ strongest lines arise from the $\delta m = 0$ transitions; each isotope has $I = 3/2$, and the less abundant isotope ^{65}Cu with the larger nuclear magnetic moment has the greater splitting. The arrows indicate "forbidden transitions," in which the nuclear magnetic quantum number changes; competition between the nuclear electric quadrupole interaction and the magnetic hyperfine interaction relaxes the selection rule $\delta m = 0$. [After Bleaney, Bowers, and Ingram (29).]

for the spin $S = 1/2$, the ground state has four-fold degeneracy. The orbital degeneracy is lifted by a change in the symmetry of the hydrated copper complex, through the Jahn-Teller effect. There is a continuous set of distortions that all give the same energy [Van Vleck (30)], and in copper fluosilicate at temperatures above about 100 K Bleaney and Ingram (31) observed a single line with an isotropic g-value, a result that was explained by Abragam and Pryce (32). Later, Bleaney and Bowers (33) found that as the temperature is lowered, the isotropic line is replaced by a spectrum corresponding to that of three ions, each in a field of tetragonal symmetry. These were the first direct observations of dynamic and static Jahn-Teller effects in the solid state.

(c) Copper acetate has an anomalous temperature variation of its susceptibility, and Bleaney and Bowers (34) found that its ESR spectrum was quite different from that of a single cupric ion. They suggested that the crystal contained pairs of copper ions with a strong exchange interaction, resulting in a singlet ground state with a triplet lying higher by about 300 cm^{-1}. The hyperfine structure of this triplet state contains 7 lines of unequal intensity, as expected for a "dimer" containing two copper ions and two nuclei, each of nuclear spin $I = 3/2$. This
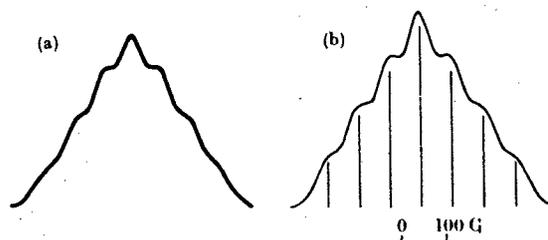

Figure 9. Measured (a) and calulated (b) hyperfine structure of copper in the triplet level of copper acetate [Bleaney and Bowers (34)]. The cupric ions occur in dimeric pairs, and the h.f.s. arises from the pair of copper nuclei, each with $I = 3/2$. The seven line h.f.s. should have intensity ratios 1:2:3:4:3:2:1.

structure is shown in Figure 9.

Measurements on neodymium ethylsulfate (35) represented the start of a comprehensive investigation of the lanthanide (4f) group, using two series of compounds, the ethylsulfates, and the double nitrates isomorphous with lanthanum magnesium nitrate. In the course of this work the nuclear spins of all the stable lanthanide isotopes were determined or confirmed, and the nature of the paramagnetism of these compounds was explained in detail. With the help of A.E.R.E., Harwell in growing radioactive single crystals of the 5f group, the spectra of neptunyl and plutonyl complexes in uranyl rubidium nitrate

were observed (36,37); the results were interpreted (38) in terms of covalent bonding involving the 5f electron, the first time that such bonding had been suggested. In addition, the nuclear spins of the isotopes ^{237}Np, ^{239}Pu, and ^{241}Pu were determined from the hyperfine structure. Measurements on trivalent uranium ions in single crystals of $LaCl_3$, initiated by Clyde A. Hutchison, Jr. at Chicago, showed that in this compound the behavior of the uranium ion closely resembles its lanthanide analogue, Nd^{3+}, $4f^3$. The nuclear spins of the isotopes ^{233}U and ^{235}U were also determined (39,40).

Extensive work on ions of the other transition groups 4d,5d was carried out by Griffiths and Owen. This confirmed the presence of covalent bonding in these compounds, as in the complex cyanides of the 3d group. The wave functions of the magnetic electrons spread out onto the ligand ions, and result in a complex hyperfine structure if the ligand ions have nuclear spins and magnetic moments. An example of such a structure is shown in Figure 10 for a dilute chloroiridate compound
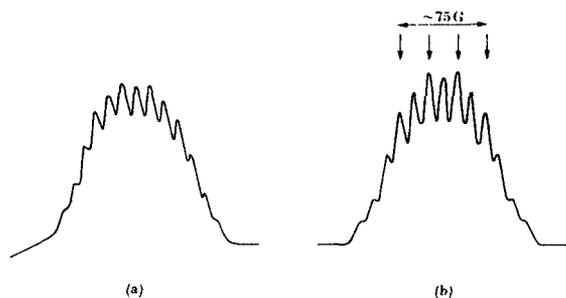

Figure 10. Complex hyperfine structure in the paramagnetic resonance spectrum of $Na_2(Ir,PtCl_6),6H_2O$; (a) observed by Griffiths and Owen (41). In the reconstruction (b), the arrows indicate the position of the four hyperfine lines of the iridium nuclei (I = 3/2); the remaining structure arises from overlap of the magnetic electrons onto the ligand chlorine nuclei (for which also I = 3/2).

(41). In addition to the four hyperfine lines of the two iridium isotopes

191 and 193 (each with I = 3/2 and almost identical nuclear magnetic moments), there is a complex of lines from the ligand chlorine nuclei.

In another application of FPR, measurements of the spectra of pairs of ions in crystals of intermediate dilution were used to determine the size and nature of the interactions between the magnetic ions [see (42)].

VII. NUCLEAR ALIGNMENT

The electron paramagnetic resonance work in the Clarendon Laboratory was of direct interest to the large low temperature group in the same department under Professor Sir Francis Simon in suggesting the best substances for magnetic cooling and temperature measurements. Cerium magnesium nitrate was investigated by Cooke, Duffus, and Wolf (43); not only did it become the standard substance for thermometry below 1 K and for cooling to millikelvin temperatures by isentropic demagnetization [Daniels and Robinson (44)], but later it was the substance in which an Orbach relaxation process was first observed by Finn, Orbach, and Wolf (45). Another important contribution arose from the discovery that the hyperfine structure of divalent cobalt in many single crystals is highly anisotropic [Bleaney and Ingram (46)]. This led to the suggestion [Bleaney (47)] that in a cobalt salt an appreciable degree of alignment of the nuclear spins would be obtained on demagnetization to zero field, and that this would be a simpler and more efficient method than that proposed by Gorter (48) and by Rose (49). Such "alignment" does not result in any net nuclear polarization, but is sufficient to produce anisotropy in the spatial emission of gamma rays. The first successful experiment was carried out by Daniels, Grace, and Robinson (50) in the autumn of 1951, using a mixed crystal of a double sulphate containing 1% cobalt, 12% copper, 87% zinc, and a trace of the radioactive cobalt-60. A temperature of about 20 mK was obtained on demagnetization, and a ratio of 1.44:1 for the rates of emission of gamma rays in two mutually perpendicular directions was observed, decaying to 1:1 as the compound warmed up

towards 1 K. Nuclear orientation, combined with the use of nuclear resonance for precise measurement of the hyperfine frequencies of radioactive isotopes, has now become a far-ranging field in its own right.

VIII. CONCLUSION

This brief survey can give only an impression of the rapid progress made in electron paramagnetic resonance in those years. This was partly due to the simplicity of the apparatus used in most of the low temperature experiments, though that then required for liquid helium temperatures was more complicated than the systems commonly used now; fortunately only a few substances had such rapid spin-lattice relaxation rates that helium temperatures were required to obtain a resonance spectrum. On the theoretical side a very important part was played by Professor M. H. L. Pryce, who realized that the interpretation of the electron paramagnetic resonance results provided an excellent area for theoretical graduate students, together with A. Abragam, K. W. H. Stevens, R. J. Elliott, M. C. M. O'Brien, B. R. Judd, and Julius Eisenstein, who wrote their doctoral theses on various features of crystal field theory, hyperfine structure, and the detailed interpretation of other aspects of paramagnetism as revealed by electron spin resonance.

REFERENCES

[1] R. H. Dicke, Rev. Sci. Inst. *17*, 268 (1946).

[2] R. H. Dicke, R. Beringer, R. L. Kyle, and A. B. Vane, Phys. Rev. *70*, 340 (1946).

[3] G. E. Becker and S. H. Autler, Phys. Rev. *70*, 300 (1946).

[4] J. H. Van Vleck and V. W. Weisskopf, Rev. Mod. Phys. *17*, 227 (1945).

[5] C. E. Cleeton and N. H. Williams, Phys. Rev. *45*, 234 (1934).

[6] B. Bleaney and R. P. Penrose, Proc. Phys. Soc. *59*, 418 (1947).

[7] B. Bleaney and R. P. Penrose, Nature *157*, 339 (1946); Proc. Roy. Sci. (London), Ser. A *189*, 358 (1947).

[8] H.-Y. Sheng, E. F. Barker, and D. M. Dennison, Phys. Rev. *60*, 786 (1941).

[9] B. Bleaney and J. H. Loubser, Nature *161*, 522 (1948); Proc. Phys. Soc. *63*, 483 (1950).

[10] B. Bleaney and R. P. Penrose, Phys. Rev. *70*, 775 (1946); Proc. Phys. Soc. *60*, 83 (1948).

[11] C. H. Townes and A. L. Schawlow, Microwave Spectroscopy, McGraw Hill Co., New York (1955).

[12] J. H. E. Griffiths, Nature *158*, 670 (1946).

[13] C. Kittel, Phys. Rev. *73*, 155 (1948).

[14] J. H. Van Vleck, Phys. Rev. *78*, 266 (1950).

[15] E. Zavoisky, Fiz. Zh. *9*, 211 (1945).

[16] D. M. S. Bagguley and J. H. E. Griffiths, Nature *160*, 532 (1947).

[17] C. J. Gorter and J. H. Van Vleck, Phys. Rev. *72*, 1126 (1947).

[18] D. M. S. Bagguley and J. H. Griffiths, Nature *162*, 538 (1948); Proc. Roy. Soc. (London), Ser. A *201*, 366 (1950).

[19] J. H. Van Vleck, Phys. Rev. *74*, 1168 (1948).

[20] M. H. L. Pryce, Nature *162*, 539 (1948).

[21] R. P. Penrose and K. W. H. Stevens, Proc. Phys. Soc. *A63*, 29 (1950).

[22] D. M. S. Bagguley, B. Bleaney, J. H. E. Griffiths, R. P. Penrose, and B. I. Plumpton, Proc. Phys. Soc. *61*, 542, 551 (1948).

[23] R. P. Penrose, Nature *163*, 992 (1949).

[24] A. Abragam and M. H. L. Pryce, Nature *163*, 993 (1949).

[25] B. Bleaney, Phys. Rev. *78*, 214 (1950).

[26] B. Bleaney and D. J. E. Ingram, Proc. Roy. Soc. (London), Ser. A *205*, 336 (1951).

[27] A. Abragam, Phys. Rev. *79*, 534 (1950); A. Abragam and M. H. L. Pryce, Proc. Roy. Soc. (London), Ser. A *206*, 164 (1951).

[28] D. J. E. Ingram, Proc. Phys. Soc. *A62*, 664 (1949).

[29] B. Bleaney, K. D. Bowers, and D. J. E. Ingram, Proc. Phys. Soc. *A64*, 758 (1951).

[30] J. H. Van Vleck, J. Chem. Phys. *7*, 72 (1939).

[31] B. Bleaney and D. J. E. Ingram, Proc. Phys. Soc. *A63*, 408 (1950).

[32] A. Abragam and M. H. L. Pryce,

Proc. Phys. Soc. *A63*, 409 (1950).

[33]B. Bleaney and K. D. Bowers, Proc. Phys. Soc. *A65*, 667 (1952).

[34]B. Bleaney and K. D. Bowers, Phil. Mag. *43*, 372 (1952); Proc. Roy. Soc. (London), Ser. A *214*, 451 (1952).

[35]B. Bleaney and H. E. D. Scovil, Proc. Phys. Soc. *A63*, 1369 (1950).

[36]B. Bleaney, P. M. LLewellyn, M. H. L. Pryce, and G. R. Hall, Phil. Mag. *45*, 992 (1954).

[37]B. Bleaney, P. M. Llewellyn, M. H. L. Pryce, and G. R. Hall, Phil. Mag. *45*, 991 (1954).

[38]J. Eisenstein and M. H. L. Pryce, Proc. Roy. Soc. (London), Ser. A *229*, 20 (1955).

[39]B. Bleaney, C. A. Hutchison Jr., P. M. LLewellyn, and D. C. D. Pope, Proc. Phys. Soc. *B69*, 1167 (1956).

[40]C. A. Hutchison Jr., P. M. Llewellyn, E. Wong, and P. Dorain, Phys. Rev. *102*, 292 (1956).

[41]J. H. E. Griffiths and J. Owen, Proc. Roy. Soc. (London), Ser. A *226*, 96 (1954).

[42]J. M. Baker and B. Bleaney, Conf. on Low Temp. Physics, Paris, 83 (1955); J. H. E. Griffiths, J. Owen, J. G. Park, and M. F. Partridge, Proc. Roy. Soc. (London), Ser. A *250*, 84 (1957); J. Owen, J. Appl. Phys. Suppl. *32*, 213S (1961).

[43]A. H. Cooke, J. H. Duffus, and W. P. Wolf, Phil. Mag. *44*, 623 (1953).

[44]J. M. Daniels and F. N. H. Robinson, Phil. Mag. *44*, 630 (1953).

[45]C. B. P. Finn, R. Orbach, and W. P. Wolf, Proc. Phys. Soc. *77*, 261 (1961).

[46]B. Bleaney and D. J. E. Ingram, Nature *164*, 116 (1949).

[47]B. Bleaney, Proc. Phys. Soc. *A64*, 315 (1951); Phil Mag. *42*, 441 (1951).

[48]C. J. Gorter, Physica *14*, 504 (1948).

[49]M. E. Rose, Phys. Rev. *75*, 213 (1949).

[50]J. M. Daniels, M. A. Grace, and F. N. H. Robinson, Nature *168*, 780 (1951); B. Bleaney, J. M. Daniels, M. A. Grace, H. Halban, N. Kurti, and F. N. H. Robinson, Phys. Rev. *85*, 688 (1952); B. Bleaney, J. M. Daniels, M. A. Grace, H. Halban, N. Kurti, F. N. H. Robinson, and F. E. Simon, Proc. Roy. Soc. (London), Ser. A *221*, 170 (1954).